# Multi-physics modeling in the electromagnetic levitation and melting of reactive metals

A. A. Roy[*], V. Bojarevics,  K.A. Pericleous
CMS, University of Greenwich
*Corresponding author:  A.A.Roy@gre.ac.uk

**Abstract:** The aim of this article is to demonstrate the capability of the software for predicting free-surface motion, internal fluid flow and temperature in an electromagnetically levitated sample of liquid metal.  Multi-physics solutions which demonstrate the usefulness of Comsol as a powerful MHD simulation tool have been generated to two industrial problems using the ALE moving-mesh module in combination with the Navier-Stokes, Maxwell and General Heat transfer modules.  The first problem, which has relevance to continuous casting of metal ingots in a cold crucible, considers the transient free-surface motion of a semi-levitated volume of metal when its shape is confined by the field of a solenoid.  The ability to establish the steady-state profile of the melt is an important factor in determining power requirements and thermal losses. This can then be fed into a 3D model (with static geometry) to include the effects of joule heating and the influence of the finger segments.  The second problem is concerned with the thermo-physical property measurement of reactive molten materials using a novel technique reported in [9].  Comsol is used to predict the surface motion, centre of mass oscillations and temperature fluctuation in a metal droplet suspended in the AC field of a solenoid.

**Keywords:** Electromagnetic levitation, MHD, free-surface

## 1. Introduction

Electromagnetic levitation has wide-ranging applications in metal processing - shape controlling, flow suppression, casting, property measurement etc. [1].   The technology relies on the use of an induction coil carrying AC current at medium/high frequency to melt and control the shape/temperature of a metal alloy (especially in an overheated state).

A well known application is that of the "cold crucible" [2] which consists of a plurality of electrically disconnected water-cooled copper segments arranged in a circle, surrounded by an induction coil.  These segments enclose the charge (typically of a titanium-based composition) which is melted by Joule heating via the induced eddy currents from the alternating magnetic field of the coils.  Magnetic forces limit the contact area between the melt and the segments thereby reducing unwanted heat loss.  The main advantage of cold-crucibles over conventional ceramic crucibles is that reactive materials can be melted with minimum contamination [3].

Section 2.1 focuses on the use of cold-crucible technology in the continuous casting of Ti metal ingots.   Scrap metal is fed (eg. with a vibrating feeder) and melted using a multi-turn water-cooled induction coil at a given rate in the "bottomless" crucible (Fig. 1).    The molten volume, which is a dome-shaped on top by the EM confinement force, is drawn downwards through a water-cooled sleeve (formed by the segments) using a mechanical withdrawal system [4].  A solidification front or "crust" develops which grows according to the rate at which heat is extracted.  The procedure is conducted within an evacuated chamber.  The same technology can be applied to casting Si ingots [6].
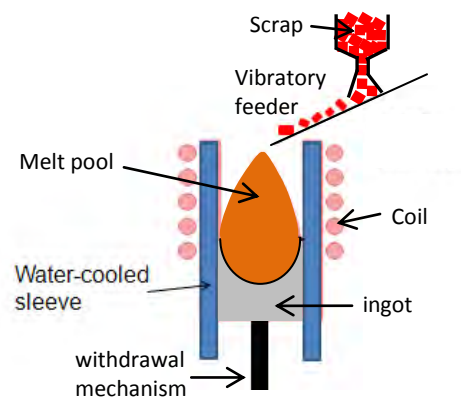


**Figure 1.** Continuous casting of metal ingots.

It is known that the field seen by the charge is largely unaffected by the presence of the

copper segments due to electromagnetic transparency [5]. Hence the steady-state shape of the molten dome can be determined approximately from a 2D axisymmetric model. We show the capability of Comsol for predicting the steady-state shape of the liquid envelope by considering the electromagnetic confinement forces on a volume of molten titanium. The moving mesh module permits dynamic adjustment of the free-surface according to the effects of surface tension and magnetic pressure. The module is coupled to the Navier Stokes and Maxwell solvers yielding a transient magneto-hydrodynamic description of the melt. The steady-state shape can then be used in a 3D model (with static geometry) to yield estimates of joule heating in the segmented crucible sections and estimates of power efficiency.

The second use of electromagnetic levitation discussed herewith is in the thermo-physical property measurement of reactive alloys. Conventional methods of studying such alloys at high temperature are difficult due to potential contamination with the measuring apparatus. Sec. 2.2 focuses on a novel technique developed originally by Wunderlich & Fecht [7] and later extended by Fukuyama[8] and Tsukada[9] for determining the thermal conductivity of a molten droplet of liquid metal. The technique involves levitating the sample in the AC field of a solenoid with a static DC magnetic field present to suppress convection. The authors assume that the droplet has a fixed spherical shape which is only an approximation in reality. With Comsol (using the moving mesh module) it is possible to predict dynamic surface deformation and axial translational motion of the droplet according to the effects of gravity, surface tension and magnetic pressure. This is important because any instability could lead to an inaccurate measurement of the thermal conductivity.

## 2. Geometry configurations

### 2.1 Cold crucible continuous casting
The geometry of one-quarter of the cold-crucible used in the continuous casting application is shown in Fig. 2. The crucible dimensions are typical for an industrial scale installation. Sixteen water cooled copper segments with radial thickness 24mm and inner radius 52mm

surround the titanium charge. The five-turn induction coil carries an effective current of 3kA at 12kHz.
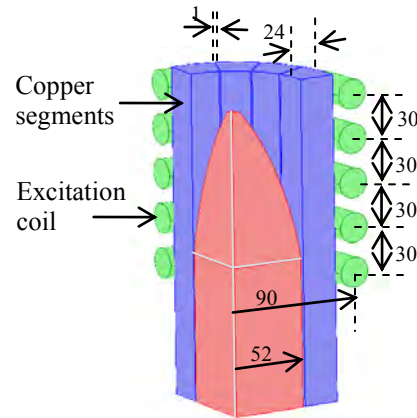


Figure 2. Cold crucible geometry.

The shape of the molten dome is a balance between the Lorentz force, gravity and surface tension. In Sec. 3 we provide a numerical description of the model for predicting the free-surface. The final steady state is then used in a 3D model with static geometry. For simplicity, we assume that there is no electrical contact between the charge and the melt and we ignore the 3D effect of coil helicity which allows us to exploit symmetry. At 12kHz the skin-depth in the copper (0.65mm) is small compared to the conductor thickness. Hence the excitation coils and finger segments can be modeled using an impedance boundary condition.

### 2.2 Thermo-physical property measurement
A contactless technique has been developed for measuring the thermal conductivity of a molten droplet of liquid metal [9]. The droplet is levitated in the AC field of the solenoid shown in Fig. 3 (note that the top two turns are counter wound with the respect to the lower turns) and its upper surface is exposed to periodic laser heating. The Lorentz force drives intense fluid flow in the turbulent regime whose magnitude is suppressed by an axial-directed static DC field (>4T). The thermal conductivity is obtained by experimentally measuring the phase shift between the waveform for the input power (from the laser) and the temperature response at the bottom of the droplet and relating this to numerical simulations.
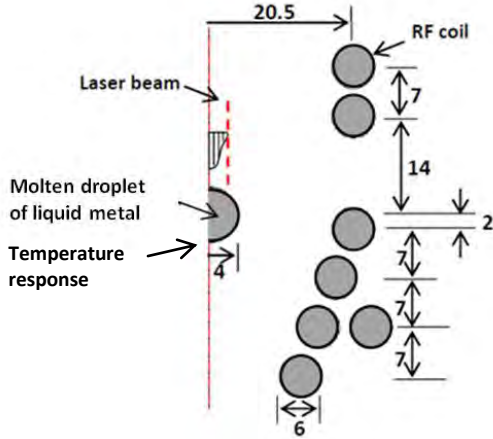
Figure 3. Experimental set-up of induction coil.

The authors assume that the droplet remains spherical. The moving mesh module is used to simulate the dynamic change in shape which occurs in a real experiment and the effect of axial translational motion on the thermal profile. The ability to predict this is important because any instability could lead to fluctuation in the temperature which could complicate the measurement of the phase shift.

## 3. Numerical Models

The MHD industrial applications described in this paper involve modelling fluid flow, heat transfer, and Maxwells equations, with dynamic free-surface adjustment. The relevant differential equations are listed below.

Incompressible Navier Stokes (transient)

$$\rho\left(\frac{\partial u}{\partial t} + (u.\nabla)u\right) = -\nabla p + \nabla.(\eta(\nabla u + \nabla u^{T}))$$
$$+ \mathrm{Re}(J \times B^{*})/2 + \rho g + F_{damp}$$

$$\nabla.u = 0$$

General Heat Transfer (transient)

$$\rho C_{p}\left(\frac{\partial T}{\partial t} + u.\nabla T\right) = \nabla.(k\nabla T) + \mathrm{Re}(E.J^{*})/2$$

Maxwells Equations (time-harmonic)

$$\nabla \times H = J + \frac{dD}{dt} \quad \nabla \times E = -\frac{dB}{dt}$$
$$B = \mu_{0}\mu_{r}H \quad J = \sigma E$$

where $\rho$ is the density, $u = (u,v)$ is the fluid velocity, $p$ is the pressure, $\eta$ is the dynamic viscosity, $C_{p}$ is the specific heat capacity, $k$ is the thermal conductivity, T is the temperature, $g$ is the acceleration due to gravity, $\sigma$ is the electrical conductivity, $\mu$ the magnetic permeability, $A$ the electromagnetic vector potential and $F_{damp}$ is the damping force (when a static axial magnetic field of strength $B_{s}$ is present). Comsol produces a time-harmonic solution of Maxwell's Equations in terms of the vector potential $A$ which satisfies $\nabla \times A = B$.

The movement and deformation of the free surface is modeled using an Arbitrary Lagrangian-Eulerian (ALE) formulation which is a hybrid combination of the classical Lagrangian and Eulerian approaches. The Lagrangian approach is useful for mechanical problems or "contained fluids" in which the boundary displacement is relatively small. Its main disadvantage lies in its inability to follow large distortions without avoiding a highly contorted mesh. The Eulerian approach is suitable for fluid flow when there are no free surfaces or moving boundaries. The ALE method combines the best features of these approaches using a moving grid whose velocity is neither zero (Eulerian) nor equal to the velocity of the fluid (Lagrangian). Instead, the velocity varies smoothly and arbitrarily between these two limits.

Surface tension is implemented according to the approach described in Carin[10] using the weak form of the boundary condition

$$[-pI + \eta(\nabla u + \nabla u^{T}].n = -P_{a}n + \Gamma\gamma n \quad (1)$$

(written more concisely in terms of the stress tensor as $\Pi_{nn} = \Gamma\gamma$, $\Pi_{\tau n = 0}$ ) where $n$ is the outward unit normal, $P_{a}$ is the surrounding pressure (= 0 in this model), $\Gamma$ is the curvature and $\gamma$ is the surface tension (assumed to be constant).

## 3.1 Modeling assumptions

### Continuous casting

This application makes use of the Navier-Stokes, AC/DC and moving mesh modules. To predict the shape and hydrodynamic behavior of the liquid envelope we must include the effect of the magnetic pressure from the field of the solenoid. The shaded region represents the portion of the melt zone which is free to deform (constrained on the base and the symmetry line).

The aximuthal component of the electromagnetic vector potential $A$ (which yields the time-averaged Lorentz force $Re(JxB^*)/2$ acting on the fluid) is solved throughout the entire domain. Pressure and velocity are solved only within the melt zone. The boundary condition (1) is imposed on the free-surface and a wall (no slip) condition on the lower face. Oscillatory behavior in the liquid envelope is damped by the effects of viscosity (chosen artificially high to account for the effects of turbulence).
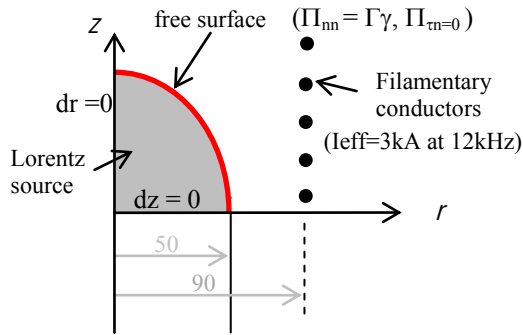


Figure 4. Geometry for prediction of free-surface.

The final 2D steady-state geometry can then be incorporated in a 3D electromagnetic model of the crucible to include the effect of the finger segments. If coil helicity is ignored we may exploit symmetry and model an appropriate wedge of the geometry. Fig. 5 was produced for the case of a crucible consisting of 16 segments and shows a single segment bordered on either side by half-an-air gap (0.5mm). The 5x1 column vector of voltage phasors needed to impose an effective current of 3kA in each turn of the coil is obtained from the 5x5 complex impedance matrix. (The complex impedance matrix is obtained by inverting the admittance matrix). These values are imposed on the cross-section of each turn (the corresponding opposite faces being earthed).
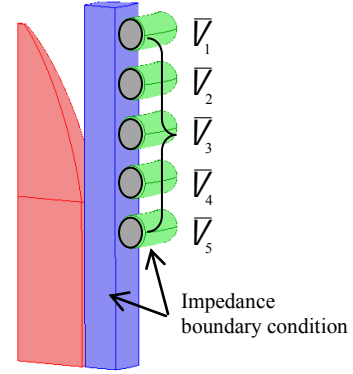


Figure 5. One wedge of the geometry.

Since the skin depth in copper at 12kHz is small (0.65mm) in relation to the thickness of the fingers (20mm) and the coil radius (8mm) we employ the "impedance boundary condition". This condition employs the 1D diffusion equation to impose the ratio E/H on the surface of the conductors. Mathematically it is written

$$Z_s^{-1}(n \times H) + E - (n.E)E = 0$$

where

$$Z_s = \sqrt{\frac{\varepsilon_0 \varepsilon_r - j\sigma/\omega}{\mu_0 \mu_r}}$$

The condition is not appropriate in the titanium because its lower conductivity (and higher skin-depth) leads to field penetration at much greater depths.

### Thermo-physical property measurement

This application makes use of the Navier Stokes, General Heat transfer, AC/DC and moving mesh modules. An effective current of 375A at 200kHz is imposed in the solenoid and the electromagnetic vector potential is solved throughout the entire domain. The solution for fluid flow and heat transfer is restricted to the computational domain of the droplet. The hydrodynamic boundary condition (1) is imposed on the surface of the droplet. Fluid flow is driven by the time-averaged Lorentz force $Re(JxB^*)/2$ but there is also a radial damping force $uB_s^2$ ($vxBxB$) due to the static

axial magnetic field $B = B_s \hat{z}$. The droplet is heated internally by the time-averaged Joule source $\mathrm{Re}(E.J^*)/2$ and externally (on its upper surface) by the modulated source from the laser. This source is Gaussian distributed and takes the form:

$$q_{laser} = \alpha \, 2 P_0 / (\pi \, r_{laser}^2)(1 + \cos \omega_{laser} \, t) \exp(-2 \, r^2 / r_{laser}^2)(e_n . e_{laser})$$

where $r_{laser}$ is the radius at which the laser intensity is less by a factor of $e^2$, $\omega_{laser}$ is the angular frequency of the beam, $\alpha_p$ is the absorptivity and $P_0$ is the beam power (related to the intensity of the laser beam on the symmetry axis).

Heat escapes from the surface of the droplet by radiation according to the condition $\varepsilon \sigma_B (T^4 - T^4_{amb})$ were $\varepsilon$ is the emissivity and $T_{amb}$ is the ambient temperature of the surroundings. The boundary conditions are summarized in Fig. 5.
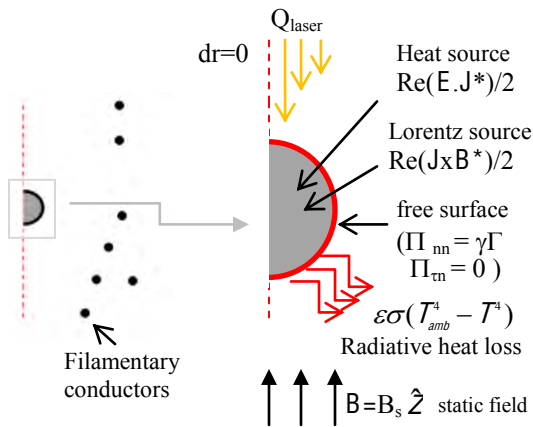


Figure 6. Boundary conditions on the droplet.

## 4. Results

### Continuous casting

Comsol was used to predict the evolution of the liquid titanium envelope for a simple test-case with Ieff=3kA at f=12kHz. Fig. 7 (left) shows the initial shape of the melt and (right) the shape after 0.1 second. [1] The zone colour describes

---

[1] While Comsol has the functionality to include Darcy resistance/solidification modeling within the frame-work of

pressure, the contours are streamlines of magnetic of flux and the arrows indicate the time-averaged Lorentz force.
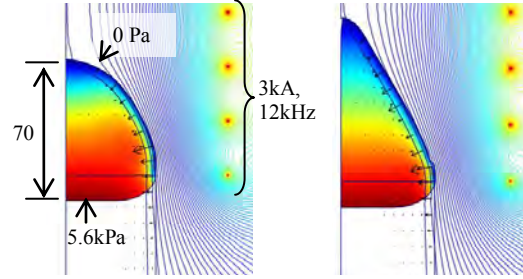


Figure 7. Surface profile: t=0 (left) and t=0.1 (right).

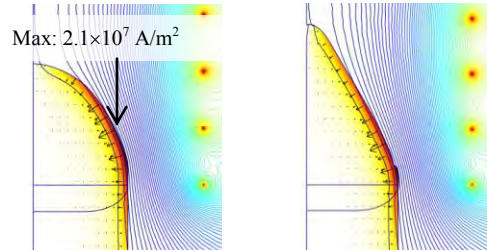Fig. 8 shows the effective current density in the melt which is confined within a skin-layer.



Figure 8. Effective current: t=0 (left) and t=0.1sec.

These results show the influence of the Lorentz force which pushes the melt inwards and upwards. As the confinement force from the coils becomes weaker the top portion of the melt continues to drift upwards (moving under its own inertia) but eventually comes to rest. Gravity causes the melt to sink downwards whereupon the confinement force from the coils becomes stronger once more and the cycle is repeated. The result is an oscillatory pattern akin to "bouncing" which is eventually damped by the effect of viscosity. The final steady-state represents a balance of surface tension, gravity and magnetic pressure. Such a steady-state profile (obtained with realistic industrial operating conditions) has been incorporated in a 3D electromagnetic model of a crucible. Fig. 9 shows a single segment bordered on either side by two half-air-gaps (this model corresponds to a wedge from a crucible consisting of eight segments).

---

continuous casting the focus of this paper is predicting the shape of the free-surface and 3D electromagnetic effects.

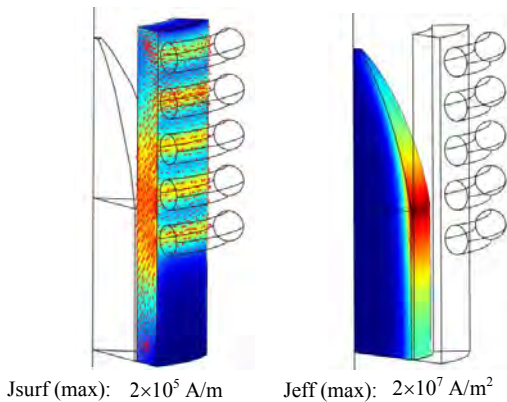Jsurf (max): $2 \times 10^5$ A/m    Jeff (max): $2 \times 10^7$ A/m$^2$

Figure 9. $J_{surf}$ on finger segment and $|J|/\sqrt{2}$ in the charge ($I_{eff}$ = 3 kA, f = 12 kHz).

On the outer surface of the fingers the induced current follows the "shadow" of the 5-turn coil whereas on the inner surface the current flows in the region which lies close to the charge. The higher surface $H$ field seen by the charge in this region leads to higher levels of joule heating. The model in Fig. 9 can be rebuilt varying the numbers of segments and gap-width to yield important information concerning power efficiency and voltage.

Thermophysical property measurement

When the droplet is released within the field of the solenoid its shape deforms in accordance with gravity, surface tension and the surrounding magnetic pressure. Typically its centre of mass will oscillate around the equilibrium position as shown in snap-shots from the simulation in Fig. 10 which shows pressure and streamlines of magnetic flux for a static magnetic field of 4T. Fig. 11 shows the corresponding temperature distribution throughout the droplet at the same set of snap-shots when the laser modulation frequency is 0.1Hz. This simulation was performed using the operating conditions reported in [9] setting the initial temperature (uniformly) throughout the droplet to 1774K. When the droplet is at its lowest axial position (t=0.2s), the pressure and temperature rise. This is because the higher $H$ field is correlated with the increase in the Lorentz force and the level of Joule heating. There is also a slight distortion in the shape at t=0.2 due to the increased "pinch" although this is less apparent to the naked eye.
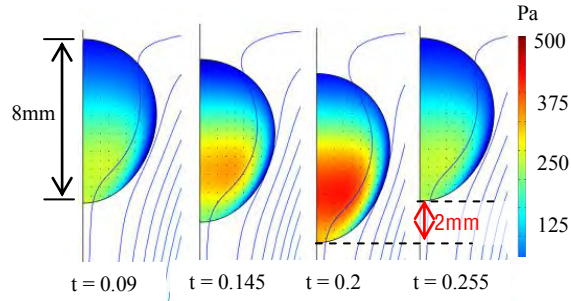


Figure 10. Pressure distribution (one oscillation).


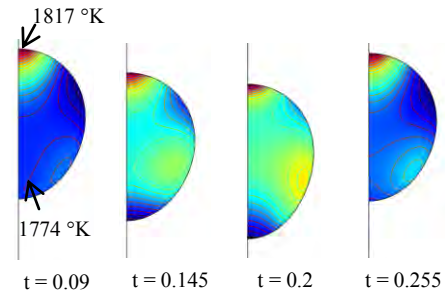
Figure 11. Temperature distribution (one oscillation).

Fig. 12 shows the $z$-displacement (mm) of the top of the droplet (red curve) and the time-averaged axial component of the Lorentz force (mN) over a time interval of one second. The droplet is initially positioned approximately 1mm below the equilibrium where it experiences an upward force of 14mN.
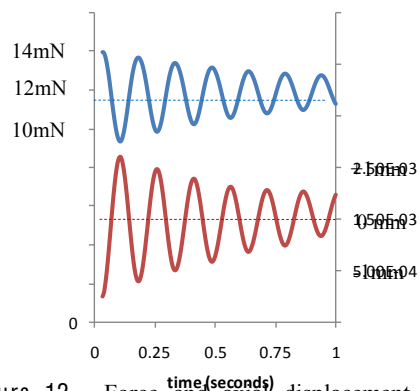


Figure 12. Force and axial displacement (1 sec interval).

The results indicate that when the axial displacement is at a maximum the Lorentz force is minimum and vice-versa. The Lorentz force

acting upwards exceeds the weight when the droplet is at its lowest position in the cycle. The opposite is true when the droplet is at the highest point in the cycle.

Fig. 13 shows the transient evolution of the temperature at the bottom polar axis of the droplet. The initial temperature (uniformly distributed) is 1774 K. The oscillations are due to the axial translational motion which cause variation in the level of Joule heating. Note that the period of each temperature oscillation (0.16sec) is much less than the period of the laser (1sec). Eventually a quasi-steady state is achieved (not shown in the present simulation).
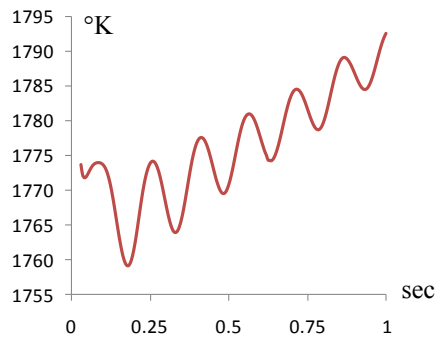


Figure 13. Temperature distribution.

## 7. Conclusions

We have demonstrated the use of Comsol as a powerful MHD simulation tool for investigating two industrial problems.

The software can provide useful information about the efficiency and design of cold crucibles – in particular for their use in continuous casting applications. It can be used to predict the 3D distribution of Joule heating on the surface of the finger segments and the total power released in the coil and charge. This has important relevance in terms of quantifying overall energy requirements and the design of the water-cooling circuit.

We have also demonstrated the use of Comsol for numerically simulating the behavior of a molten droplet of liquid metal suspended in the field of a solenoid. In particular we have shown

how temperature fluctuations in the sample can be related to axial translational motion. This has important relevance to the recently developed experimental technique reported in [9]. The ability to predict the temperature waveform at the bottom polar axis of the droplet in the presence of axial instability is important in terms of quantifying effects which could disrupt the measurement of the thermal conductivity.

## 8. References

1. Asai S., Challenging of EPM in economic production, nano-technology and environment protection. In: *Proc 4th Int Conf. Electromag. Proc. Mat.*, Lyon 1-8

2. Bojarevics V & Pericleous K.A, Numerical Modelling for the Electromagnetic Processing of Materials, In: *Magnetohydrodynamics: Historical Evolution and Trends*, Springer (2006)

3. Bojarevics V. et al., Modeling the dynamics of magnetic semi-levitation melting, *Met and Mat Trans.*, 31B, 179-189 (2000)

4. Tanaka T. et al.; Continuous casting of titanium alloy by an induction cold crucible, ISIJ Inter. 32, 5, 575-582 (1992)

5. Westphal, E. et al. Electromagnetic field distribution in an induction furnace with cold crucible, *Mag, IEEE Trans.* 32, 1601-1604 (1996)

6. Nakagawa K., Manufacturing of silicon ingot in electromagnetic casting, In: *5th Inter. Symp. on Electromag. Proc. of Mat.*, 773-777 (2006)

7. Wunderlich R., Fecht H., Meas. Sci. Technol. 16, 402-416 (2005)

8. H. Fukuyama et al. Meas. Sci. Technol. 18, 2059-2066 (2007),

9. T. Tsukada, H. Fukuyama, H. Kobatake, Int. J. Heat Mass Transfer 50, 3054-3061 (2007)

10. M. Carin, Square drop oscillation under surface tension – www.comsol.com